Characterization and Theory of Electrocatalysts Based on Scanning Electrochemical Microscopy Screening Methods†

José L. Fernández,‡ J. Michael White, Yangming Sun, Wenjie Tang, Graeme Henkelman, and Allen J. Bard*

Department of Chemistry and Biochemistry, The University of Texas at Austin, Austin, Texas 78712

Received April 28, 2006. In Final Form: July 27, 2006

A strategy for finding new electrocatalysts for the oxygen reduction reaction (ORR) in acidic solutions is outlined and illustrated with results for Pd−Co catalysts. This is based on establishing guidelines for selecting test systems, rapid preparation of arrays, and rapid screening by scanning electrochemical microscopy. Promising candidates are further tested as supported electrocatalysts by larger scale electrochemical methods and in fuel cells, with optimization of the composition and structure. Those that emerge are characterized by a variety of methods, including X-ray diffraction, scanning electron microscopy, and X-ray photoemission spectroscopy. Finally, density functional theory is used for detailed calculations of oxygen adsorption and dissociation on the material and provides better guidelines for further testing.

The ultimate adoption of fuel cells as power sources depends strongly on their cost and efficiency. A key factor in both of these issues is the fuel cell cathode where the oxygen reduction reaction (ORR) occurs and important questions about whether the currently favored electrocatalyst for polymer electrolyte membrane fuel cells (PEMFC), Pt supported on C, is a viable option.[1,2,3] The cost of Pt and the limited world supply are significant barriers to the widespread use of PEMFC. Moreover, most of the power lost in a fuel cell at reasonable operating currents occurs at the cathode (>0.4 V at practical current densities), even with high loadings of Pt in the electrocatalyst. We, as well as many others, have been engaged in a search for non-platinum-based cathode materials and in obtaining a better understanding about guidelines for selecting materials to test for this purpose, i.e., the replacement of platinum with a less-expensive metal that also plays a synergetic role (e.g., Co, Ni, Ti).[4−8] Another approach to this problem is to design new metal combinations that do not contain Pt but metals less expensive and with catalytic activity at least equal to that in Pt; [9,10] some additional general references to fuel cells and to earlier work in this area have been given in a recent paper.[11] Because of the large number of possible elementary steps and mechanistic routes in the reduction of O_2 to H_2O, the detailed mechanism of the ORR, even at Pt, is still controversial.[12]

The approach we have taken is based on the following steps:

1. Find guidelines to aid in the selection of materials for investigation, e.g., bimetallic and trimetallic catalysts.

2. Devise synthetic approaches for the rapid preparation of electrocatalyst test arrays of different composition on a conductive substrate, e.g., glassy carbon.

3. Use the scanning electrochemical microscopy (SECM) approach to test the arrays in strongly acidic media and to select promising candidate materials.

4. Optimize synthetic methods (e.g., by water-in-oil microemulsion or template methods), prepare carbon-supported catalysts with these and test with a rotating disk electrode (RDE) configuration.

5. Prepare fuel cell catalysts and test in PEMFC for efficiency and lifetime under actual operating conditions.

6. Characterize good materials (e.g., by XRD, SEM, and XPS) to obtain a better understanding of their composition (particle size, oxidation state...).

7. Carry out theoretical studies of the catalyst to improve models for how they work and for new material selection.

In this paper, we briefly provide an overview of the results of items 1−5 as they apply to electrocatalysts of Pd and Co, which have been some of the most successful ones. We mainly deal with items 6 and 7, the characterization of Pd−Co and theoretical models for its behavior in the ORR. Several theoretical approaches that involve quantum chemical calculations (e.g., ASED-MO, DFT) have been applied in recent years to predict the relationship between the nature of the catalyst surface and ORR activity on transition metals, mainly Pt.[13−20] In these treatments, the interaction between molecular oxygen and the surface metal atoms is considered assuming possible reaction pathways and energies. Recent reports show that the ORR activity

† Part of the Electrochemistry special issue.

* To whom correspondence should be addressed.

‡ Current address: Facultad de Ingeniería Química, Universidad Nacional del Litoral, Santa Fe, Argentina.

(1) Ralph, T. R.; Hogarth, M. P. *Platinum Metals Rev.* **2002**, *46*, 3.
(2) Aricò, A. S.; Srinivasan, S.; Antonucci, V. *Fuel Cells* **2001**, *1*, 133.
(3) Steele, B. C. H.; Heinzel, A. *Nature* **2001**, *414*, 345.
(4) Mukerjee, S.; Srinivasan, S. *J. Electroanal. Chem.* **1993**, *357*, 201.
(5) Antolini, E.; Passos, R. R.; Ticianelli, E. A. *Electrochim. Acta* **2002**, *48*, 263.
(6) Xiong, L.; Manthiram, A. *Electrochim. Acta* **2004**, *49*, 4163.
(7) Shim, J.; Lee, C.-R.; Lee, H.-K.; Lee, J.-S.; Cairns, E. J. *J. Power Sources* **2001**, *102*, 172.
(8) Shao, M.-H.; Sasaki, K.; Adzic, R. R. *J. Am. Chem. Soc.* **2006**, *128*, 3526.
(9) Rivera-Noriega, R.; Castillo-Hernández, N.; Soto-Guzman, A. B.; Solorza-Feria, O. *Int. J. Hydrogen Energy* **2002**, *27*, 457.
(10) Ye, S.; Vijh, A. K. *Electrochem. Commun.* **2003**, *5*, 272.
(11) Raghuveer, V.; Manthiram, A.; Bard, A. J. *J. Phys. Chem. B* **2005**, *109*, 22909.
(12) Adzic, R. In *Electrocatalysis*; Lipkowski, J., Ross, P. N., Eds.; Wiley-VCH: New York, 1998; Chapter 5, p 197.
(13) Anderson, A. B.; Albu, T. V. *J. Electrochem. Soc.* **2000**, *147*, 4229.
(14) Anderson, A. B. *Electrochim. Acta* **2002**, *47*, 3759.
(15) Balbuena, P. B.; Altomare, D.; Vadlamani, N.; Bingi, S.; Agapito, L. A.; Seminario, J. M. *J. Phys. Chem. A* **2004**, *108*, 6378.
(16) Wang, Y.; Balbuena, P. B. *J. Phys. Chem. B* **2005**, *109*, 14896.
(17) Wang, Y.; Balbuena, P. B. *J. Phys. Chem. B* **2005**, *109*, 18902.
(18) Xu, Y.; Ruban, A. V.; Mavrikakis, M. *J. Am. Chem. Soc.* **2004**, *126*, 4717.
(19) Greeley, J.; Mavrikakis, M. *Nat. Mater.* **2004**, *3*, 810.
(20) Nørskov, J. K.; Rossmeisl, J.; Logadottir, A.; Lindqvist, L.; Kitchin, J. R.; Bligaard, T.; Jónsson, H. *J. Phys. Chem. B* **2004**, *108*, 17886.

10.1021/la061164h CCC: $33.50
Published on Web 09/27/2006

is related to the strength of the metal−oxide (M−O) bond,[20] which relates to an adsorbed oxygen atom as an ORR intermediate. Metals with very negative oxygen binding energy easily cleave molecular oxygen but subsequently form strong inert oxides and therefore have an inappropriate (not sufficiently positive) cathode potential. Metals with very positive oxygen binding energy, such as Ag and Au, are noble and have a high barrier for the dissociative adsorption of oxygen, so they also tend to be poor ORR catalysts. Platinum is the best transition metal ORR catalyst, having the optimal balance between being able to both cleave and reduce oxygen. In this context, a rational design of improved multimetallic ORR catalysts, for example, by the combination of a noble metal with a second metal, was proposed as a guiding mechanistic principle that needs to be supported by detailed quantum chemistry calculations. For example, recent theoretical calculations have suggested a synergetic mechanism for a Pt−Co alloy, in which Co forms subsurface alloys on Pt(111) leaving a Pt skin on the surface. This skin is, in fact, proposed to be more noble than Pt, bringing the alloy closer to the maximum-activity peak of the volcano curve and therefore more catalytically active.[18,19]

Experimental Section

Chemicals. $(NH_4)_2PdCl_4$ (Aldrich, Milwaukee, WI), $Co(NO_3)_2$-$(H_2O)_6$ (Aldrich), $NaBH_4$ (Aldrich), glycerol (Alfa Aesar), and sulfuric acid (98 wt %, Alfa Aesar) were all of reagent grade and were used as received. Reagent solutions were prepared using Milli-Q water. Glassy carbon plates (1 mm thick) and Vulcan XC-72R carbon black were purchased from Alfa Aesar and Cabot, respectively.

Preparation of Pd−Co Catalyst Spots. Two different types of Pd−Co catalyst spots were analyzed, which are identified as samples A and B, respectively.

Sample A was a Pd−Co (80 at. % Pd) spot deposited on a glassy carbon plate by reduction of metal salts with hydrogen by a procedure similar to that described for preparation of catalyst spot arrays. Briefly, 0.1 μL (a single drop of near 1 mm diameter) of a solution of the metal salts (ammonium tetrachloropalladate and cobalt nitrate) containing 0.3 M metal in water−glycerol (3:1) was deposited on a glassy carbon plate using a micropipet. The drop was dried at 150 °C under argon for 30 min and immediately reduced under hydrogen (1 atm) at 350 °C for 1 h using a tube furnace (Barnstead International, Dubuque, IA). The resulting metal spot was rinsed with water.

Sample B was a Pd−Co (80 at. % Pd) spot after operation as oxygen cathode in acidic medium. A spot prepared identically to sample A was immersed in O_2-saturated 0.5 M H_2SO_4 solution and polarized at 0.2 V vs a hydrogen reference electrode for a 2 h duration. Under these conditions, the Pd−Co spot catalyzes the 4-electron reduction of O_2 to water under mass-transfer control. The spot was then thoroughly rinsed with water and dried in air.

Preparation of Carbon Supported Pd-Alloy Electrocatalysts. Carbon-supported Pd−Co catalyst with a metal loading of 20 wt % was prepared by the borohydride method. The required amounts of metal salts (ammonium tetrachloropalladate and cobalt nitrate) were added to a constantly stirring carbon slurry prepared by suspending 160 mg of Vulcan XC-72R carbon black in 100 mL of deionized water. This suspension was agitated in an ultrasonic water bath at room temperature for 30 min. A few drops of 1 M NaOH solution were then added to this mixture to raise the pH to 10 before adding 10 mL of a 5 wt % sodium borohydride solution. The resulting reaction mixture was stirred for 15 min, allowed stand overnight, and filtered. The carbon-supported catalyst was thoroughly washed with deionized water and dried in air. A final thermal treatment at 350 °C in Ar for 1 h was applied to the catalyst. To prepare the sample for surface and compositional analysis, 10 mg of the catalyst were suspended in 1 mL of ethanol using an ultrasonic bath. A 0.1 μL drop of this suspension was deposited onto a glassy carbon plate and dried in air at 80 °C. This sample is identified in this work as sample C.

Compositional and Surface Analysis. Localized compositional analysis of the Pd−Co catalyst spots were carried out using energy dispersive spectroscopic (EDS) analysis in a scanning electron microscope. EDS analysis and SEM images were performed using a LEO 1530 scanning electron microscope equipped with an IXRF EDS system, the latter operated with a 10 kV electron beam and 60 μm aperture (average counts ranging from 1500 to 2000 s^{-1}). For XPS analysis, spectra were taken on a PHI 5700 XPS system using a monochromatic Al X-ray source operated at pass energies of 117.4 eV for surveys and 11.7 eV for high-resolution scans. The binding energy was calibrated using Au4f, Cu2p, and Ag3d.

Results and Discussion

Array Synthesis and SECM Screening. A recent report from our group[21] proposed a guiding principle for the design of non-platinum electrocatalysts for the ORR that focuses on the metal oxide route to oxygen reduction (i.e., the direct four-electron route) that was later further refined by DFT calculations.[17] This pathway involves closely pairing a good oxygen-bond cleaving metal (e.g., Co) for first splitting of the O−O bond to form adsorbed oxygen, with a good metal (e.g., Pd) for efficient reduction of adsorbed oxygen atoms, which are then reduced to water. In this synergetic mechanism applied for example to the Pd−Co alloy, molecular oxygen binds to a surface cobalt atom and dissociatively adsorbs into the neighboring hollow sites on the alloy surface. The character of these hollow sites is dominated by palladium so that the oxygen atoms are readily reduced to form water.

Following these thermodynamic guidelines, several bimetallic combinations that should verify increased electrocatalytic activity for the ORR were prepared and tested.[21,22] A rapid SECM-based technique allowed a preliminary ORR activity test of the proposed combinations over a range of possible compositions to be carried out. Thus, selected groups of bimetallic materials and ranges of compositions that showed clear synergetic effects were identified and later prepared and evaluated under conditions closer to those in PEMFC. These experiments probed that alloys of Pd and Au with Co, V, and Ti can catalyze the ORR as efficiently and even better than Pt.[21−23] This selection and testing process is summarized in Figure 1 for the case of Pd−Co combinations.[21] The ORR SECM activity maps of Pd−Co spots presented in Figure 1a detected alloys of Pd−Co with 10−20 at. % Co that could efficiently catalyze the electroreduction of oxygen at overpotentials (η) where no activity is observed for pure Pd. Carbon-supported PEMFC-type electrodes were fabricated with these Pd−Co combinations and evaluated in rotating disk experiments (Figure 1b), where it was verified that they also are good oxygen cathodes when the metals are supported on carbon, with a performance that can even compete with Pt.

Surface and Compositional Analysis of Sample A (Array Spot Before Use). The Pd−Co spot (80 at. % Pd in the precursor solution) obtained by thermal reduction at 350 °C with H_2 was investigated by SEM with simultaneous EDS analysis and mapping of the Pd and Co compositions. Figure 2-I shows (a) the SEM micrographs and corresponding Pd (b) and Co (c) EDS maps, and Table 1 summarizes the measured compositions. Additional SEM micrographs can be seen in Figure SI1 of the Supporting Information. The spot is inhomogeneous in morphology and in composition, with Pd-rich (97 at. % Pd) and Co-rich (40 at. % Pd) regions. The phase diagram of the Pd−Co binary

(21) Fernández, J. L.; Walsh, D. A.; Bard, A. J. *J. Am. Chem. Soc.* **2005**, *127*, 357.
(22) Walsh, D. A.; Fernández, J. L.; Bard, A. J. *J. Electrochem. Soc.* **2006**, *153*, E99.
(23) Fernández, J. L.; Raghuveer, V.; Manthiram, A.; Bard, A. J. *J. Am. Chem. Soc.* **2005**, *127*, 13100.

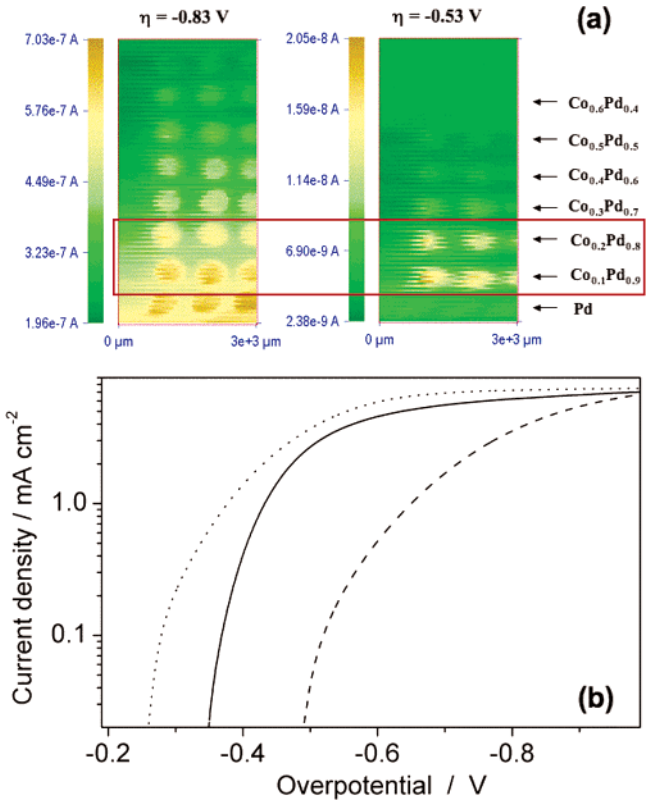

Figure 1. (a) SECM tip generation-substrate collection images of ORR activity measured on Pd−Co binary arrays in 0.5 M H_2SO_4. Tip−substrate distance = 30 μm, tip current = −160 nA, scan rate = 50 μm each 0.2 s. (b) Polarization curves of carbon black-supported 20 wt % Pd−Co with 20 at. % Co (solid line), Pd (dashed line), and Pt (dotted line) rotating disk electrodes in O_2-saturated (1 atm) 0.5 M H_2SO_4. Rotation rate: 2000 rpm (adapted from ref 21).

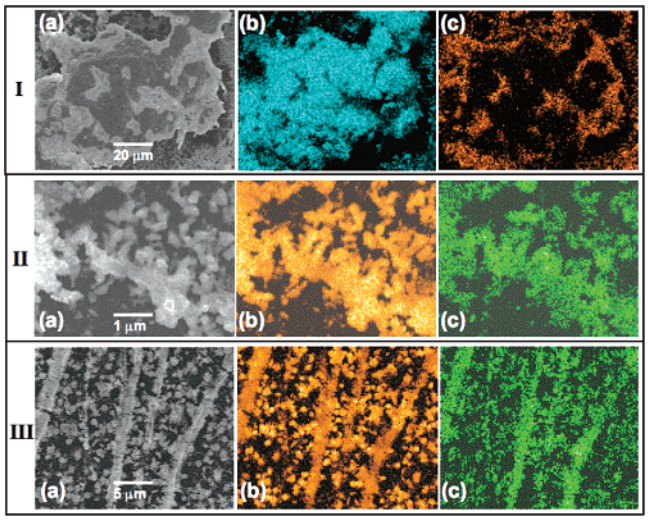

Figure 2. (I) SEM micrographs (a), Pd (b), and Co (c) EDS composition maps of sample A. (II and III) SEM micrographs (a), Pd (b), and Co (c) EDS composition maps of sample B obtained on two regions with different morphologies.

system at this temperature indicates the formation of an fcc solid solution and of a Co-rich cph solid solution, but the equilibrium between these two phases is unknown.[24] Thus, both phases are expected to be present in the spot, and the ratio between them is controlled by the fast evaporation of the precursor solution,

(24) Ishida, K.; Nishizawa, T. In *Binary Alloy Phase Diagrams*; Massalski, T., Okamoto, H., Subramanian, P. R., Kacprzak, L., Eds.; ASM International: Materials Park, OH, 1990; pp 1222−1224.

Table 1. Compositions Measured by EDS and XPS on Pd−Co Catalysts

	at. % Pd				
	sample A			sample B	sample C
EDS	Pd-rich 97.1	Co-rich 40.4	mean value 68.8	74.0	80.2
XPS	edge area 68.0	central area 51.0	mean value 59.5	78.3	67.8

as well as the temperature and time of the thermal reduction treatment, which probably was not sufficient to attain complete homogenization by solid-state reorganization of the components. The XPS spectra of the spot around the Co2p and Pd3d signals are shown in Figure 3-I (spectrum i). According to the binding energy of these signals, Pd is metallic (335.4 eV) while Co is found as a mixture of metal and oxide (778.3 and 780.4 eV, respectively). The mean surface composition is more concentrated in Co (40 at. % Co) than the bulk composition measured by EDS (30 at. % Co), indicating segregation of Co toward the surface. After a short treatment of the surface by etching of a few atomic layers with an Ar^+ beam, the XPS analysis shows that the peak intensities of both Pd3d and Co2p increased (spectra ii), which resulted from the removal of contaminants adsorbed on the surface. Moreover, after surface cleaning, the ratio of metallic Co to oxidized Co increased significantly, demonstrating that oxidized Co is concentrated at the surface.

Surface and Compositional Analysis of Sample B (Array Spot After Use As Oxygen Cathode). SEM and EDS studies were performed on a Pd−Co spot that operated as an oxygen cathode in the acidic medium. The SEM micrographs of the spots at low magnification (Figure SI2 in Supporting Information) show more pronounced morphological nonuniformity than that observed in the spot before the use for the ORR. However, the SEM micrographs and corresponding Pd and Co EDS analysis shown in Figure 2-II and 2-III indicate that the spot is homogeneous in composition. There is only one Pd-rich phase with about 74 at. % Pd (see Table 1), which indicates that the Co-rich phase detected in the as-prepared spot (sample A) dissolved during the ORR at the spot in acid solution. Thus, the remaining phase is probably an fcc Pd−Co solid solution. From the analysis of the Co2p and Pd3d binding energy values observed in the XPS spectra of the spot (not shown), these signals are seen to be generated from metallic palladium (335.4 eV) and cobalt oxide (780.4 eV). In contrast to the as-prepared sample, no signal corresponding to metallic cobalt was observed. Moreover, the surface composition (78 at. % Pd) is similar to that measured by EDS (74 at. % Pd), which indicates that segregation of Co was diminished.

Surface and Compositional Analysis of Sample C (Unused Sample Supported on Carbon). EDS analysis was performed on a spot made with carbon black-supported Pd−Co nanoparticles prepared by chemical reduction of metal precursors with sodium borohydride. This analysis showed uniform distribution of components, which indicates the existence of a single phase, most likely an fcc Pd−Co solid solution with a mean concentration of 80.2 at. % Pd (see Table 1). The similarity between this value and the metal concentration in the precursor solution is the consequence of a slow and more controlled method for the preparation of the alloy compared to the array spots. Surface analysis by XPS (Figure 3-II) indicated that Pd is metallic, while Co is fully oxidized, and that there is some segregation of Co toward the surface (68 at. % Pd).

Calculations of Oxygen Dissociation on a Co/Pd(111) Surface. The hypotheses that make the foundations of our proposed rules for predicting ORR synergetic effects between

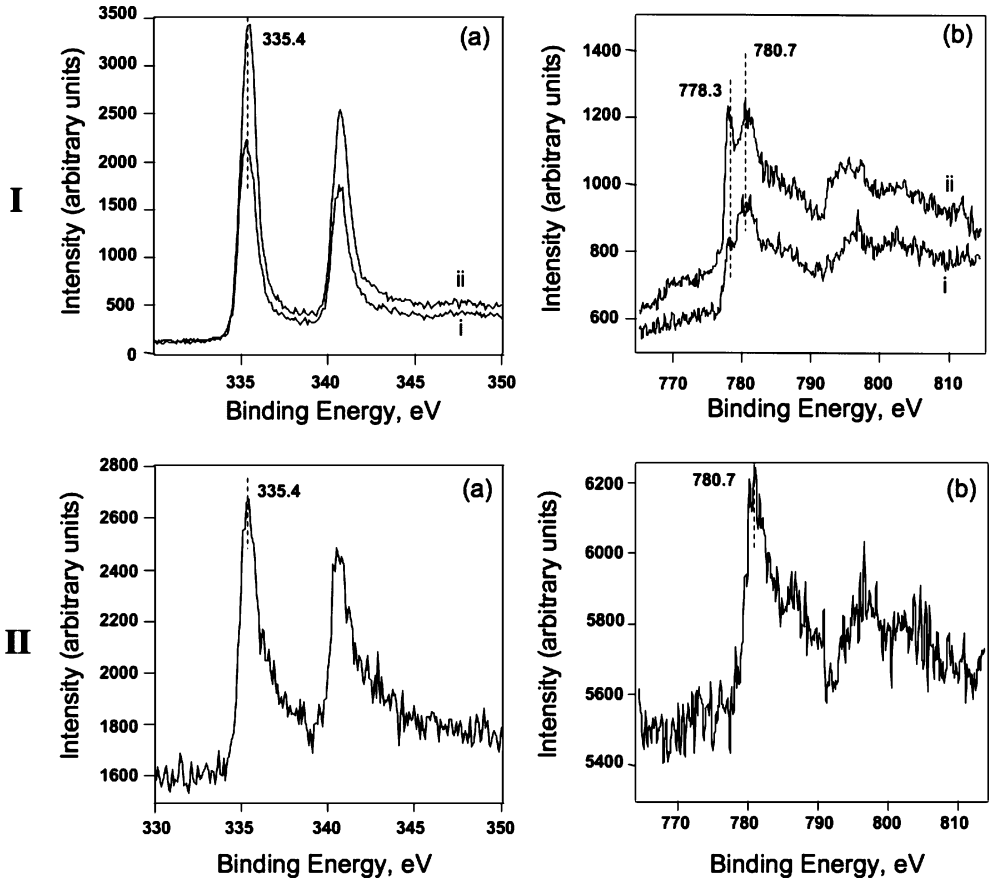

Figure 3. (I) XPS spectra around Pd3d (a) and Co2p (b) signals of sample A as prepared (i) and after cleaning with an Ar^+ beam (ii). (II) XPS spectra around Pd3d (a) and Co2p (b) signals of sample C.

two metals are intuitive and are based upon thermodynamic data of bulk materials. Such a model may not be suitable to describe the bimetallic surface behavior. Moreover, there are several factors that are not taken into account in this simplified model and compromise the predictions. The surface atomic structure of the alloy could clearly be a very important factor for predicting activity, and bonding between metal atoms may also result in alloy properties that are more complicated than just a combination of their individual properties. Catalytic reactions can also take place at surface defects such as step and kink sites. The formation of intermediates, such as hydroxyl, could also dominate the kinetics, or these could bind irreversibly to oxygen cleavage sites.[20] However, even when it is clear that the proposed guidelines are based on an oversimplified model, they have succeeded in leading to improved catalysts.

To make these guidelines more rigorous and to understand in more detail how and why this principle works and when it fails, it is necessary to make a more precise description of the metal catalyst surface by quantum chemistry calculations. These calculations permit one to form a more realistic picture of the surface reaction processes, to establish their feasibility, and to obtain quantitative thermodynamic information.

In this context, to better understand how the addition of Co to Pd affects the ORR, we have used density functional theory (DFT) calculations to compare the mechanism and barrier of O_2 dissociative adsorption on a model Pd(111) surface, with a surface containing Co. All DFT calculations were done with the PW91 functional[25] using the generalized gradient approximation as implemented in the VASP code.[26,27] Valance electrons were treated explicitly in the Kohn−Sham equations,[28] and core

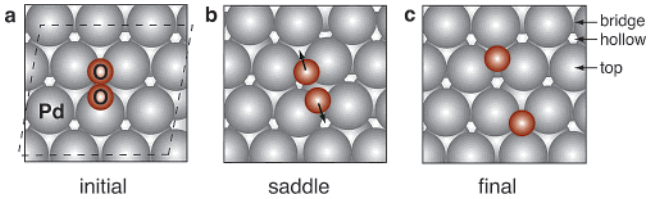

Figure 4. Mechanism of O_2 dissociation on Pd(111). Molecular oxygen binds to the surface with an energy of 1.47 eV in a top−hollow−bridge (t-h-b) geometry (a). The mechanism of dissociation has both O atoms crossing bridge sites at the saddle point (b). The energy barrier for dissociation is found to be 0.37 eV. In the final, dissociated state (c), both O atoms have moved to different hollow sites than initially occupied by the O_2 molecule.

electrons were incorporated into pseudopotentials with the projector augmented-wave (PAW) method.[29,30] All calculations included spin-polarization, which was found to be important for the surfaces with Co and adsorbed O.

The Pd(111) catalyst surface was modeled as a four-layer periodic slab containing nine atoms per layer. The atoms in the bottom two Pd layers were held at the DFT lattice constant of 3.97 Å, which is a few percent larger than the experimental value of 3.89 Å. These lower atoms were held frozen in all calculations. The 3×3 unit cell in the plane of the slab is outlined in Figure 4a. The Brillouin zone was sampled with a $2 \times 2 \times 1$ Monkhosrt−Pack *k*-point mesh[31] and a plane wave basis set cutoff of 268 eV was used. The energetics of oxygen dissociation was not found

(25) Perdew, J. P.; Wang, Y. *Phys. Rev. B* **1992**, *45*, 13244.

(26) Kresse, G. *Phys. Rev. B* **2000** *62*, 8295.
(27) Kresse, G.; Hafner, J. *Surf. Sci.* **2000**, *459*, 287.
(28) Kresse, G.; Furthmuller, J. *Comput. Mater. Sci.* **1996**, *6*, 15.
(29) Blochl, P. E. *Phys. Rev. B* **1994**, *50*, 17953.
(30) Kresse, G.; Joubert, J. *Phys. Rev. B* **1999**, *59*, 1758.
(31) Monkhorst, H. J.; Pack, J. D. *Phys. Rev. B* **1976**, *13*, 5188.

to change significantly upon increasing the *k*-point mesh to 3 × 3 × 1 or using a higher plane wave cutoff of 400 eV.

Our calculations show that molecular oxygen binds in the hollow site on Pd(111) aligned in a top−hollow−bridge (t-h-b) geometry. The binding energy of O_2 is 1.47 eV, taken with respect to the gas-phase molecule. A Bader analysis[32,33] shows that 0.73 electrons are transferred to the O_2 molecule when adsorbed on the surface. This strong electronic interaction indicates that the O_2 molecule chemically adsorbs to the metal surface. The molecular adsorption geometry is consistent with what has been found in previous calculations.[37]

The reaction pathway for O_2 dissociation was found using the nudged elastic band method.[34] In this method, a set of images is used to connect the initial (molecularly adsorbed) state with a final (dissociated) state. Typically, eight images are used to resolve the pathway, which is optimized to trace out the minimum-energy path connecting the chosen endpoints. A climbing-image algorithm[35] was used to ensure that the highest energy image along the path rigorously converges to the saddle point. Subsequent optimizations of the saddle point (for example, using a finer *k*-point mesh or upon addition of Co) were done using the dimer method.[36] This minimum mode following method takes an initial geometry to a nearby saddle point, without needing to specify the reaction pathway. A minimization was done from each calculated saddle point to verify the geometry of the associated initial and final states.

The reaction mechanism for O_2 dissociation has both O atoms crossing bridge sites into hollow sites (see Figure 4). At the saddle point, the 'top' atom from the (t-h-b) molecular state moves to a bridge site in an adjacent hollow (see Figure 4b). This is interesting because the O atoms dissociate into hollow sites that are well separated (by two sites) on the Pd surface (see Figure 4c). This is different from the mechanism of O_2 dissociation that has been previously reported on Pd[37] and Pt,[18] in which each O atom dissociates to an adjacent hollow.

The addition of Co to the Pd surface does not qualitatively change the O_2 absorption geometry or dissociation mechanism, but the energy landscape is very different. We have modeled this by adding one Co atom to the Pd surface layer. The addition of one Co atom in nine atoms gives a surface concentration of 11%. A comparison of the O_2 dissociation landscape on $Pd_{1.0}$ and $Pd_{0.89}Co_{0.11}$ is shown in Figure 5. The inset figures show the geometry of oxygen on the Co-doped surface, although they are very similar to those on pure Pd, as shown in Figure 4. These same configurations are shown schematically along the reaction coordinate axis.

The O_2 molecule has a binding energy of 2.76 eV at the Co atom (Figure 5a); 1.29 eV stronger than on Pd. The Co atom lowers the saddle point energy by even more, reducing the 0.37 eV dissociation barrier on Pd to a negligible 0.01 eV. The dissociated state (Figure 5b) is also lower in energy because one O atom is bound strongly at a hollow site next to the Co atom. By removing each of the individual O atoms from the surface, we find that the strong binding in the dissociated state (Figure 5b) can be decomposed into a binding energy of 2.63 eV for the

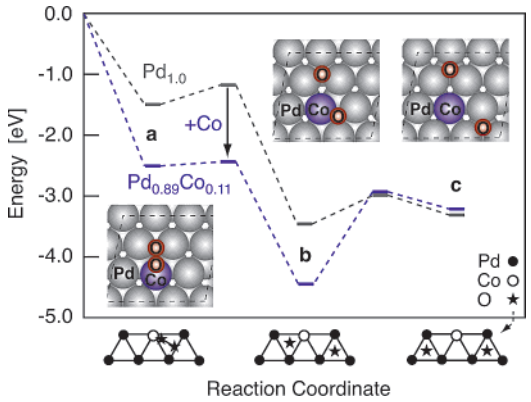

Figure 5. Energy pathway for the dissociation of O_2 on Pd(111) (upper gray curve) and upon addition of 11% Co in the surface layer (lower blue curve). O_2 binds in a hollow site next to the Co atom (a) with a binding energy 1.29 eV stronger than on pure Pd. The energy barrier for dissociation drops from 0.37 to 0.01 eV in the presence of a surface Co atom. Dissociation leaves one O bound near the Co atom, and the other in a Pd hollow site (b). The 1.50 eV energy barrier for O diffusion (b to c) in the presence of a Co atom shows that O binds irreversibly to Co. Each O atom has a binding energy of 1.84 eV in a Pd hollow site adjacent to the Co hollow (c). This is similar to the binding energy of 1.79 eV on the Pd surface, indicating that the Co−O interaction is short ranged.

O atom adjacent the Co and 1.84 eV for the O atom in the Pd hollow site. This later binding energy is similar to that of O on pure Pd, 1.79 eV, showing that the Co has a very localized interaction with O. This dissociated state is metastable; when both O atoms sit in hollow sites next to the Co atom, the binding energy is 2.52 eV per O atom.

A good catalyst strikes a balance between lowering the saddle point energy without increasing the binding energy of the products so much as to make further reactions energetically unfavorable.[38] It appears that a single Co atom on the surface of Pd is enough to swing this balance toward strong product binding. To determine how difficult it is for the Co-bound oxygen to further react, we have continued the reaction coordinate in Figure 5 by a diffusion step (from Figure 5b to c). On Pd (upper curve), an O atom diffuses between hollow sites with a barrier of 0.28 eV, but for an O atom to diffuse away from Co (lower curve), it must break the strong Co−O bond. This barrier of 1.50 eV is too high to overcome at room temperature, so that one of the O atoms binds irreversibly to Co as the O_2 is cleaved. The other O atom, however, dissociates into a hollow site surrounded by Pd atoms and can be reduced as on pure Pd if the reduction rate is faster than diffusion back to the Co atom.

This O_2 dissociation mechanism at Co into a neighboring Pd hollow site could explain the observation that 10−20% Co alloyed with Pd is best ratio for an ORR catalyst. A single Co atom essentially eliminates the barrier for O_2 cleavage. There should, however, be enough Co on the surface to maximum the number of such cleavage sites. However, once the Co concentration becomes too high, there will be few hollow sites, made up of three Pd atoms, for the O atoms to cleave into. A perfect array of Co atoms in every fourth site on the surface would be ideal (25% Co), but as a random alloy, one would expect the optimal concentration (maximizing the number of active Co sites surrounded by Pd hollow sites) to be lower.

Since surface Co will oxidize irreversibly during the ORR, it is important to investigate the equilibrium oxidation state of the metal surface during catalysis. A full investigation is beyond the

(32) Bader, R. *Atoms in Molecules: A Quantum Theory*; Oxford University Press: New York, 1990.
(33) Henkelman, G.; Arnaldsson, A.; Jónsson, H. *Comput. Mater. Sci.* **2006**, *36*, 354.
(34) Jónsson, H.; Mills, G.; Jacobsen, K. W. In *Classical and Quantum Dynamics in Condensed Phase Simulations*; Berne, B. J., Ciccotti, G., Coker D. F., Eds.; World Scientific: Singapore, 1998; p 385.
(35) Henkelman, G.; Uberuaga, B. P.; Jónsson, H. *J. Chem. Phys.* **2000**, *113*, 9901.
(36) Henkelman, G.; Jónsson, H. *J. Chem. Phys.* **1999**, *111*, 7010.
(37) Eichler, A.; Mittendorfer, F.; Hafner J. *Phys. Rev. B* **2000**, *62*, 4744.
(38) Bligaard, T.; Nørskov, J. K.; Dahl, S.; Matthiesen, J.; Christensen, C. H.; Sehested. J. *Surf. Sci.* **2004** *224*, 206.

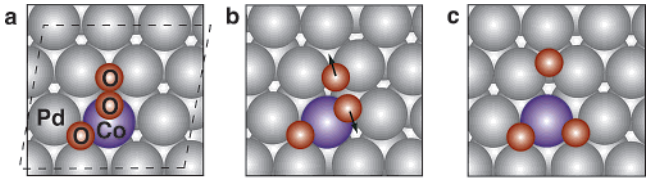

Figure 6. O_2 is found to dissociate at a Co atom in the presence of an adsorbed O atom. Surprisingly, there is no barrier for O_2 dissociation at this partially oxidized Co atom. These calculations suggest that the ORR catalytic activity takes place on a partially oxidized surface.

scope of this work, but we have started by determining if another O_2 molecule can dissociate at the Co atom after an O atom is bound irreversibly in the hollow site next to it. What we find is illustrated in Figure 6. When a second O_2 molecule is placed in a t-h-b site (Figure 6a), the molecule spontaneously dissociates (Figure 6b and c). This suggests that the active form of the Pd/Co catalyst involves oxidized Co in or on the Pd surface, in agreement with the surface analysis of sample B described above.

Another possible structure of the active Pd/Co catalyst has been suggested in which the Co atoms occupy subsurface sites below a Pd skin.[18,19] The strong Co−Pd bonds favor subsurface Co and serve to make the Pd skin more noble and perhaps better as an ORR catalysts. We have calculated that the binding energy of Co is 1.14 eV larger in a subsurface site as compared to a surface site. This energy difference will drive Co subsurface. It is possible, however, that in the presence of O, the strong Co−O bonds will keep Co on the surface. A single O atom binds next to a Co atom 1.00 eV stronger than in a pure Pd hollow site, so that it is iso-energetic to move Co from the surface to a subsurface site in the presence of an O atom. With two O atoms, Co favors the surface.

These computations are for a gas-phase system and do not include the effects of water, solvent ions, or changing potentials of the electrode surface. It is interesting, however, that they roughly give the same kind of picture of the ORR that one finds in the primitive thermodynamic approach that was originally used to select the Pd−Co system.

Conclusions

A low-cost efficient catalyst for the ORR remains to be discovered but is a key factor in the widespread deployment of PEMFC. We believe the strategy and results outlined here are useful in making progress toward this goal.

Acknowledgment. This work has been supported by the National Science Foundation Grant No. CHE 0451494. J.L.F. thanks the Fundación Antorchas Argentina for a postdoctoral fellowship. G.H. gratefully acknowledges support from the Welch Foundation under Grant No. F-1601 and the Texas Advanced Computing Center.

Supporting Information Available: Additional SEM micrographs. This material is available free of charge via the Internet at http://pubs.acs.org.

LA061164H